available at www.sciencedirect.com

ScienceDirect

journal homepage: www.elsevier.com/locate/biochempharm

Microarray analysis of hepatic gene expression in pyrazole-mediated hepatotoxicity: Identification of potential stimuli of *Cyp2a5* induction

Kathleen D. Nichols, Gordon M. Kirby *

Department of Biomedical Sciences, University of Guelph, Guelph, Ontario, Canada N1G 2W1

ARTICLE INFO

Article history:
Received 8 August 2007
Accepted 7 September 2007

Keywords:
CYP2A5
Pyrazole
Microarray
Gene expression
Hepatotoxicity
Regulation

ABSTRACT

Cytochrome P450 2a5 (*Cyp2a5*) expression is induced during liver damage caused by hepatotoxins such as pyrazole, however, the mechanism underlying this overexpression is unclear. In order to identify pathophysiological and cellular responses to pyrazole that might alter *Cyp2a5* expression, we examined the effect of pyrazole on mouse hepatic gene expression in C57BL/6 mice using Affymetrix 430 2.0 microarrays. Over 3000 differentially expressed genes were identified 24-h after pyrazole treatment that were associated with a variety of cellular pathways. Upregulated genes were primarily involved in the splicing and processing of RNA and the unfolded protein response pathway, while downregulated genes were associated with amino acid and lipid metabolism, and generation of precursor metabolites for energy production. We also examined the effects of pyrazole on cellular pathways linked to metabolic and histopathological changes observed with pyrazole toxicity. Increased mRNA levels were observed for genes involved in bilirubin production, whereas the major genes of the urea cycle were strongly decreased. Changes in genes involved in carbohydrate metabolism were also observed which could explain pyrazole-induced glycogen depletion and decreased serum glucose. In addition, over 100 genes involved in the cellular stress response were upregulated by pyrazole treatment, including genes involved in the unfolded protein response and redox status. Based on these results and previous evidence concerning the regulation of *Cyp2a5*, we have identified several pathophysiological changes including altered energy homeostasis, hyperbilirubinemia, ER stress, and altered redox status that are associated with CYP2A5 overexpression and may represent potential stimuli for the induction of *Cyp2a5*.

* *Corresponding author*. Tel.: +1 519 824 4120x54948; fax: +1 519 767 1450.
E-mail address: gkirby@uoguelph.ca (G.M. Kirby).

Abbreviations: AMPK, AMP-activated protein kinase; CYP, cytochrome P450; Gclc, glutamate-cysteine ligase catalytic subunit; GAPDH, glyceraldehyde 3-phosphate dehydrogenase; GK, glucokinase; Gpx, glutathione peroxidase; Gsr, glutathione reductase; GST, glutathione S-transferase; Gys2, glycogen synthase 2; Hmox-1, heme oxygenase; HnRNPA1, heterogeneous nuclear ribonucleoprotein A1; mOGG1, murine oxyguanine glycosylase; Nqo1, NAD(P)H quinone oxidoreductase; Pck1, phosphoenolpyruvate carboxykinase 1; Nrf2, NF-E2-related factor-2; PYR, pyrazole; Sod2, superoxide dismutase; Srxn1, sulfiredoxin.

0006-2952/$ – see front matter
doi:10.1016/j.bcp.2007.09.009

1. Introduction

Cytochrome P450 2A5 (CYP2A5), the mouse ortholog of human CYP2A6, is the major catalyst of coumarin 7-hydroxylation in the liver. High levels of the enzyme have been correlated with increased metabolism of nicotine, *N*-nitrosodiethylamine (NDEA), the tobacco-specific carcinogen NNK, and aflatoxin B1 [1–4]. Increased expression of CYP2A5 occurs during conditions typically associated with CYP downregulation including viral, fulminant, and bacterial hepatitis [5], certain tumors [6], and following treatment with a variety of structurally unrelated chemicals including hepatotoxins, heavy metals, and porphyrinogenic agents [7]. Despite this unusual expression, a common mechanism responsible for this induction has not yet been identified.

Pyrazole is a nitrogen heterocycle that strongly upregulates CYP2A5 expression at the mRNA, protein and activity levels, primarily by mRNA stabilization [8]. Pyrazole was originally investigated as a treatment for alcohol abuse due to its ability to inhibit alcohol dehydrogenase, but its usefulness has been limited by its toxicity. Acute administration of pyrazole has been shown to reduce the activity of the microsomal ethanol-oxidizing system, and to inhibit catalase activity up to 90% [9]. Acute exposure has also been shown to decrease serum glucose and urea [9], to increase bilirubin content [9], and to cause glycogen depletion in pericentral hepatocytes [10]. Ultrastructural changes including increased smooth endoplasmic reticulum, reduced rough endoplasmic reticulum, swelling of the mitochondria, and lipid accumulation have also been observed [9,10]. Although pyrazole is currently used in mechanistic studies of the regulation of CYP2A5 and CYP2E1, the cellular effects of pyrazole and its mechanism of hepatotoxicity remain poorly understood.

To gain insight into the molecular mechanisms underlying pyrazole toxicity and the upregulation of *Cyp2a5*, we utilized a microarray approach which allowed us to observe the global effects of pyrazole on hepatic gene expression. The first goal of this study was to examine the effects of pyrazole on hepatic gene expression to identify expression changes that might explain metabolic and histological changes that are observed with pyrazole treatment. The second goal was to utilize the gene expression patterns to identify potential stimuli for the induction of CYP2A5. Our results indicate that pyrazole affects the expression of over 3000 genes in diverse cellular pathways, and that many of the cellular effects of pyrazole may result from altered metabolic gene expression at the mRNA level. In addition, based on the major pathways affected by pyrazole treatment, several stimuli have been identified that should be investigated for their role in the regulation of CYP2A5 including impaired energy homeostasis, hyperbilirubinemia, ER stress, and redox imbalance.

2. Methods

2.1. Mouse treatment

C57BL/6 mice were purchased from Charles River Canada (St. Constant, QC). All mice were given food and water *ad libitum*, and were housed at 23 °C with a 12-h photoperiod. All mouse treatments were conducted in accordance with the guidelines of the Canadian Council on Animal Care and the Animal Care Committee of the University of Guelph. Eight-week-old mice were treated with a single intraperitoneal injection of either pyrazole (200 mg/kg) or saline, with four mice in each treatment group. Twenty-four hours later, mice were euthanized by CO_2 gas and serum and liver samples were collected. Serum samples were analyzed for alanine aminotransferase (ALT), cholesterol, glucose, total bilirubin, and urea (BUN) levels by the Clinical Pathology lab at the University of Guelph using an automated Hitachi 911 Bioanalyzer (Roche, Indianapolis, IN). Hepatic glycogen content was also examined in paraffin-embedded tissue sections using periodic acid-Schiff (PAS) staining according to the manufacturer's instructions (Sigma–Aldrich, St. Louis, MO). Specificity of the PAS stain for glycogen was confirmed by digesting glycogen in serial tissue sections with salivary diastase for 20 min prior to PAS staining.

2.2. Microarray assay

Gene expression profiles for liver tissue isolated from control and pyrazole-treated mice were compared by microarray analysis using Affymetrix Mouse Genome 430 2.0 arrays (Affymetrix, Santa Clara, CA). Total RNA was isolated using TRIzol reagent (Invitrogen, Burlington, ON) according to the manufacturer's protocol, and stored at −80 °C. Total RNA was then submitted to the University Health Network Microarray Centre (Toronto, Canada), where RNA quality was analyzed using an Agilent 2100 Bioanalyzer, and cRNA was generated and labelled using the one-cycle target labelling method. cRNA from each mouse was hybridized to a single array according to standard Affymetrix protocols, for a total of eight arrays. Initial image analysis of the microarray chips was performed with Affymetrix GCOS 1.4 software.

2.3. Microarray data analysis and statistics

The GeneSifter® microarray data analysis system (VizX Labs LLC, Seattle, WA, USA; http://www.genesifter.net) was used to analyze data generated in this study. This program identifies differentially expressed genes and establishes the biological significance based on Gene Ontology (GO) Consortium (http://www.geneontology.org/GO.doc.html) and KEGG public pathway resource (http://www.systems-biology.org/001/001.html). The CEL files for each array were uploaded into GeneSifter® and the data was normalized and log-transformed using the GC-RMA algorithm [11]. Differentially expressed genes were identified using Student's *t*-test (two-tailed, unpaired) and a threshold of 2.0 was used to limit the data set to genes upregulated or downregulated 2-fold or greater. Correction for multiple testing was then performed using the Benjamini–Hochberg method [12] to derive a false discovery rate estimate from the raw *p*-values. A false discovery rate of 5% was used as a cutoff for statistical significance.

The biological process ontologies and KEGG pathway terms associated with the differentially expressed genes were examined using a z-score report. The z-score was derived by subtracting the expected number of genes in a GO term meeting the criterion from the observed number of genes, and dividing by the standard deviation of the observed number of

genes, under a hypergeometric distribution. A positive z-score indicates that more genes than expected fulfilled the criterion in a certain group or pathway; therefore, that group or pathway is likely to be affected [13].

2.4. Real-time RT-PCR

Real-time PCR was utilized to confirm the differential expression of selected genes in order to confirm the quality of the microarray results. Sense and anti-sense primers were designed by using Primer3 v3.0 Software (http://frodo.wi.mit.edu/). Messenger RNA analysis was conducted by relative real-time reverse transcription-polymerase chain reaction (RT-PCR) using a Roche Molecular Biochemicals (Indianapolis, IN) Lightcycler instrument and the DNA Master SYBR Green I kit (Roche Diagnostics, Mississauga, ON). One microgram of RNA was treated with 1 unit of DNase (RQ1 RNase-Free DNase; Promega, Madison, WI), and was reverse-transcribed using 0.1 μg of random primers, 20 units of RNase inhibitor (RNasin; Promega, Madison, WI), and 200 units of Murine-Moloney Leukemia Virus reverse transcriptase (M-MLV RT). PCR was performed in a 10 μL volume containing 1 μL of SYBR Green I, 2 mM Mg^+, and 5 μM of each primer. The PCR parameters were as follows: denaturation (95 °C for 10 min), followed by 45 cycles of PCR (95 °C, 15 s; 70 °C, 5 s; 72 °C, 15 s). The threshold cycle at which the fluorescent signal reached an arbitrarily set threshold near the middle of the log-linear phase of amplification for each reaction was calculated and relative quantities of each mRNA were determined. Gene specific primers were designed to cross introns in order prevent amplification of genomic DNA contamination, and melting curve analysis was performed to confirm the presence of a single product for each primer set. All mRNA levels were normalized against mRNA levels of the housekeeping gene GAPDH. Primer set sequences and the location of the primers on the cDNA are as follows:

Cyp2a5
Forward 5′-GGACAAAGAGTTCCTGTCACTGCTTC-3′ (606–631)
Reverse 5′-GTGTTCCACTTTCTTGGTTATGAAGTCC-3′ (759–786)
GAPDH
Forward 5′-ACAGTCCATGCCATCACTGCC-3′ (581–601)
Reverse 5′-GCCTGCTTCACCACCTTCTTG-3′ (826–846)
Gclc
Forward 5′-GCATCAGGCTGTCTGCACCA-3′ (411–430)
Reverse 5′-TCCGATGCCGGATGTTTCTT-3′ (570–589)
GK
Forward 5′-GCACACGTGGTGCTTTTGAG-3′ (974–993)
Reverse 5′-GCCTTCGGTCCCCAGAGT-3′ (1020–1039)
GPx2
Forward 5′-GAGGCAGGGCTGTGCTGATT-3′ (211–230)
Reverse 5′-CACCCCCAGGTCGGACATAC-3′ (392–411)
GSTa1
Forward 5′-AAGATGGGAATTTGATGTTTGACC-3′ (204–227)
Reverse 5′-TTCTCTTTGGTCTGGGGGACA-3′ (401–421)
GSTm1
Forward 5′-TGGTTTGCAGGGGACAAGGT-3′ (637–656)
Reverse 5′-TCCAGTGGGCCATCTTTGAA-3′ (825–844)
Gys2
Forward 5′-CCAGCTTGACAAGTTCGACA-3′ (835–854)
Reverse 5′-ATCAGGCTTCCTCTTCAGCA-3′ (975–994)
Hmox-1
Forward 5′-TAAGCTGGTGATGGCTTCCTTG-3′ (269–288)
Reverse 5′-GGGATGATTTCCTGCCAGTG-3′ (426–445)
mOGG1
Forward 5′-GGCTGGTCCAGAAGCAGAGA-3′ (776–796)
Reverse 5′-GGGCCATTAAGCAGATGCAG-3′ (971–990)
Pck1
Forward 5′-TGTCGGAAGAGGACTTTGAGAAA-3′ (490–512)
Reverse 5′-TGCTGAATGGGATGACATACATG-3′ (554–576)
Nqo1
Forward 5′-GGCCGATTCAGAGTGGCATC-3′ (716–736)
Reverse 5′-AACAGGCTGCTTGGAGCAAAA-3′ (873–893)
Srxn1
Forward 5′-AACGTACCAATCGCCGTGCT-3′ (138–157)
Reverse 5′-GGCAGCCCCCAAAGGAATAG-3′ (290–309)

2.5. Immunohistochemistry

CYP2A5 protein expression was confirmed and localized in 5 μm sections of formalin-fixed, paraffin-embedded mouse liver as previously described [10]. To visualize CYP2A5 protein, slides were incubated for 2 h at room temperature with chicken anti-mouse CYP2A5 (1:1000) polyclonal antibody, followed by 1 h at room temperature with biotinylated goat antiserum to chicken immunoglobulin (Vectastain Elite ABC Kit, Vector Laboratories, Mississauga, ON). Sections were then incubated with biotinylated avidin horse-radish peroxidase, followed by final color development with hydrogen peroxide-activated 0.1% diaminobenzidine tetrahydrochloride (Sigma–Aldrich Canada Ltd., Oakville, ON) in 0.1 M Tris buffer pH 7.2 for 1 min. Sections were counterstained with Mayer's hematoxylin (Sigma–Aldrich Canada Ltd., Oakville, ON) diluted 1:1 in phosphate-buffered saline. Tissue sections were also stained with hematoxylin and eosin (H&E) according to standard staining protocols.

3. Results

3.1. Biochemical and morphological effects of pyrazole

The biochemical effects of pyrazole-mediated hepatotoxicity were determined by measuring ALT, glucose, cholesterol, total

Table 1 – Effects of pyrazole on serum biochemistry

Test (units)	Saline	Pyrazole	*p*-Value
ALT (U/L)	9.7 ± 0.9	167.0 ± 26.2*	0.027
Glucose (mmol/L)	18.9 ± 1.1	8.2 ± 1.0*	0.002
Cholesterol (mmol/L)	3.0 ± 0.2	2.9 ± 0.2	0.576
Urea (mmol/L)	5.8 ± 0.1	4.4 ± 0.4*	0.026

Serum was collected from mice 24 h following intraperitoneal administration of 200 mg/kg pyrazole or saline and was analyzed for alanine aminotransferase (ALT), glucose, cholesterol, and urea (BUN) content using a Hitachi 911 Bioanalyzer. Each value represents the average value for the samples from four mice.
* Values are significantly different from saline, $p < 0.05$ (unpaired t-test).

bilirubin, and urea levels in serum samples collected 24 h after pyrazole treatment. Pyrazole-treated mice had a 17-fold increase in serum ALT ($p < 0.05$), whereas glucose levels decreased more than 2-fold and urea showed a slight decrease of 1.4-fold following treatment ($p < 0.05$) (Table 1). No change was observed in cholesterol levels, and the effects of pyrazole on bilirubin levels could not be accurately determined since levels were below the limit of detection of the analyzer for most mice.

Hepatic glycogen content was analyzed by PAS staining of formalin-fixed paraffin-embedded liver tissue sections. Control sections from saline-treated mice demonstrated a high abundance of glycogen with a relatively uniform distribution throughout the liver (Fig. 1). The PAS staining was eliminated by diastase digestion, indicating that the stained regions represented glycogen deposits. Pyrazole treatment caused hepatic glycogen depletion in pericentral regions that were coincident with CYP2A5 overexpression (Fig. 1).

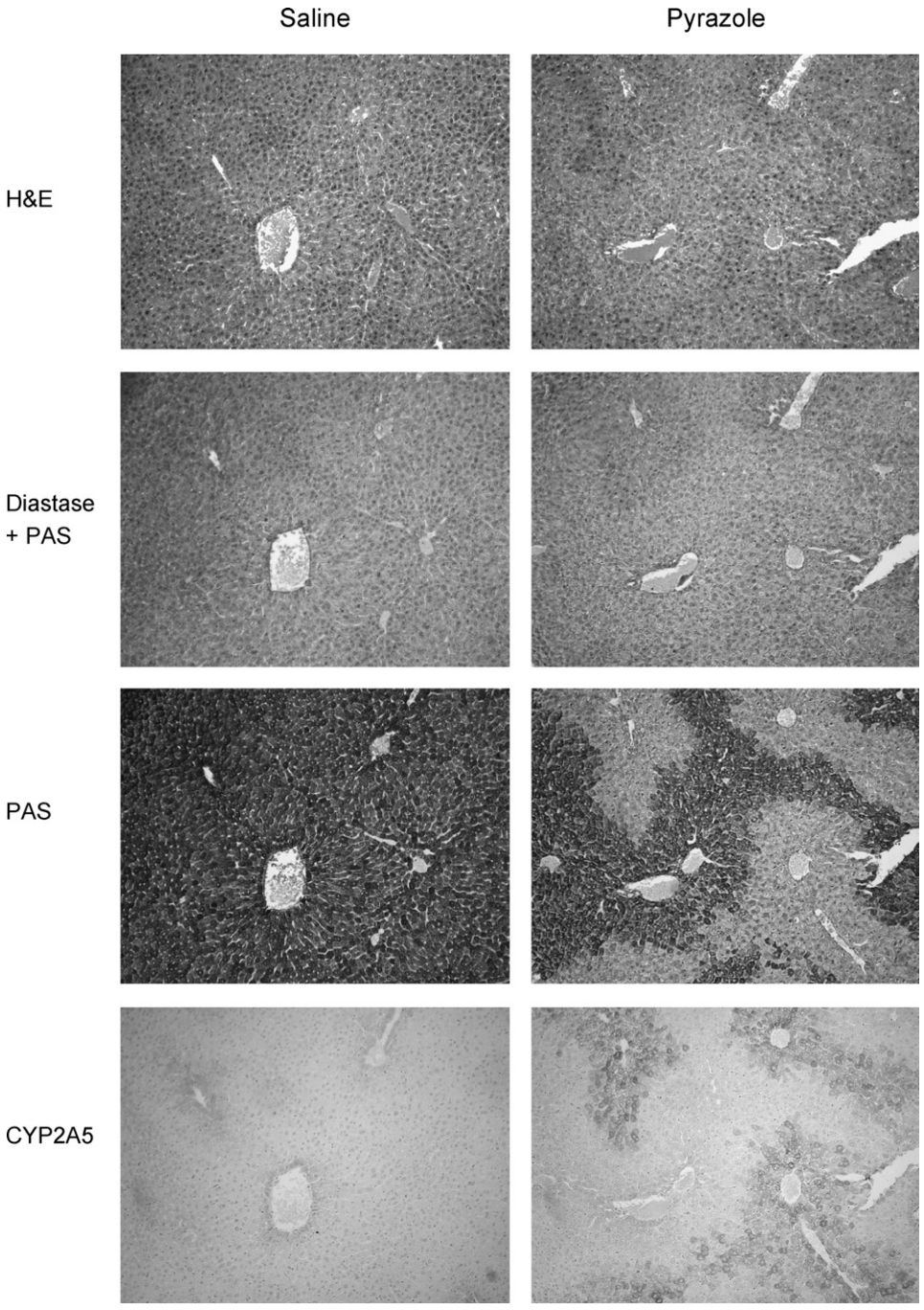

Fig. 1 – Pyrazole treatment causes glycogen depletion in pericentral hepatocytes. Mice were treated with pyrazole (200 mg/kg) or saline for 24 h and stained with hematoxylin and eosin, diastase followed by periodic acid-Schiff's reagent, periodic acid-Schiff reagent alone, or immunostained for CYP2A5. Note the co-localization of reduced glycogen content and increased CYP2A5 expression in pyrazole-treated mice. Original magnification 100×.

Table 2 – Genes with the greatest upregulation or downregulation following pyrazole treatment

Unigene	Gene symbol	Gene name	Fold change	Function
Mm.18742	Nupr1	Nuclear protein 1	+651.9	DNA binding protein involved in defense against cellular stress
Mm.13849	Hspb1	Heat shock protein 1	+220.9	Stress protein
Mm.331191	Sprr1a	Small proline-rich protein 1A	+110.0	Protection against stress
Mm.211704	Serpina7	Serine (or cysteine) peptidase inhibitor, clade A (alpha-1 antiproteinase, antitrypsin), member 7	+94.4	Carrier for thyroid hormone
Mm.218639	Srxn1	Sulfiredoxin 1 homolog (*S. cerevisiae*)	+72.0	Oxidative stress resistance
Mm.4512	Cbr3	Carbonyl reductase 3	+52.7	NADPH-dependent oxidoreductase
Mm.289936	Psat1	Phosphoserine aminotransferase 1	+48.9	Amino acid biosynthesis
Mm.197422	Gsta1	Glutathione S-transferase, alpha 1 (Ya)	+41.5	Detoxification of products of oxidative stress
Mm.275878	Derl3	Der1-like domain family, member 3	+40.6	Degradation of misfolded glycoproteins
Mm.18939	Pmm1	Phosphomannomutase 1	+35.5	Involved in glycosylation
Mm.200370	Upp2	Uridine phosphorylase 2	−132.3	Pyrimidine metabolism
Mm.24222	Sphk2	Sphingosine kinase 2	−122.0	Sphingolipid metabolism
Mm.378235	Dbp	D site albumin promoter binding protein	−56.0	Transcriptional activator—regulates clock genes
Mm.300	Car3	Carbonic anhydrase 3	−53.4	pH homeostasis—hydration of CO_2
Mm.197689	Clec2h	C-type lectin domain family 2, member h	−31.5	Unknown
Mm.14435	Hsd3b6	Hydroxy-delta-5-steroid dehydrogenase, 3 beta- and steroid delta-isomerase 6	−25.1	Steroid biosynthesis
Mm.272770	Usp2	Ubiquitin specific peptidase 2	−24.2	Ubiquitin cycle
Mm.158717	Hsd3b3	Hydroxy-delta-5-steroid dehydrogenase, 3 beta- and steroid delta-isomerase 3	−23.8	Steroid biosynthesis
Mm.196405	Hsd3b2	Hydroxy-delta-5-steroid dehydrogenase, 3 beta- and steroid delta-isomerase 2	−22.9	Steroid biosynthesis
Mm.2661	Tk1	Thymidine kinase 1	−21.8	Pyrimidine metabolism

The 10 genes with the greatest increase or decrease in expression following pyrazole treatment are listed ($p < 0.0001$). All fold changes are relative to saline controls.

3.2. *Pyrazole regulation of overall hepatic gene expression*

Analysis of log-transformed data showed that pyrazole had a highly significant and very extensive effect on gene expression in hepatic tissue. Pyrazole administration significantly ($p < 0.0001$) altered the expression of 1204 genes greater than 2-fold, resulting in upregulation of 779 genes and downregulation of 429 genes. Moreover, pyrazole induced a marked increase in the expression of certain genes, such as those encoding nuclear protein 1 and heat shock protein 1 (>200-fold), and a marked decrease in others (e.g. uridine phosphorylase, >100-fold). Indeed, pyrazole treatment was associated with a 10-fold or greater elevation in the expression of 50 genes, and an attenuation of 10-fold or more in the expression of 23 genes at this level of significance. Those genes that demonstrated the greatest change in expression with pyrazole treatment are listed in Table 2.

In order to fully characterize the biological processes associated with these gene expression changes, the criterion for "significant change" was relaxed to a p-value of <0.05. This alteration enlarged the list of genes that respond to pyrazole treatment to 3381, with an upregulation and downregulation of 2267 and 1114 genes, respectively. Although this larger list may contain some false positives, it allows for a greater opportunity to identify pyrazole-associated biological pathways by searching for enrichment in specific gene ontology designations. Furthermore, the false positives should not provide systematic contributions to any particular ontology category.

Evaluation of the larger list of genes demonstrated that pyrazole treatment has a considerable impact on a wide array of biological processes, molecular functions and cellular components in the liver. The 30 biological process ontologies with the highest z-scores for upregulated and downregulated genes are shown in Tables 3 and 4. The *primary biological processes* affected by pyrazole treatment for the upregulated genes included RNA processing, response to unfolded proteins, and intracellular transport. The downregulated genes were primarily involved in amino acid and lipid metabolism as well as generation of precursor metabolites for energy production, and electron transport. The *molecular function ontologies* most affected included RNA binding (z = 9.52) and unfolded protein binding (z = 8.04) for the upregulated genes and oxidoreductase activity (z = 13.53) and catalytic activity (z = 10.95) for the downregulated genes. Cellular components associated with upregulated genes included the nucleolus (z = 10.86), nucleus (z = 10.40), cytoplasm (z = 7.78), proteosome complex (z = 7.53), and endoplasmic reticulum (z = 6.76). Downregulated genes were primarily associated with mitochondria (z = 10.20), microsomes (z = 9.26), the endoplasmic reticulum (z = 5.63), and peroxisomes (z = 5.56).

3.3. *Effects of pyrazole on specific cellular pathways*

Since previous research in this lab [10,14] and others [9] has associated pyrazole treatment with hypoglycaemia, glycogen depletion, decreased urea nitrogen, mild hyperbilirubinemia, markers of ER stress, and oxidative damage, we examined

Table 3 – Biological process ontologies for upregulated genes

Ontology	List	Up	Down	Array	z-up	z-down
RNA processing	104	101	3	346	12.1	−3.4
Ribonucleoprotein complex Biogenesis and assembly	63	59	4	179	10.3	−1.6
rRNA processing	26	26	0	50	9.9	−1.6
rRNA metabolic process	26	26	0	51	9.8	−1.6
Response to protein stimulus	28	27	1	61	8.9	−1.1
Response to unfolded protein	28	27	1	61	8.9	−1.1
Ribosome biogenesis and assembly	35	34	1	101	7.9	−1.8
tRNA processing	20	19	1	43	7.5	−0.7
Protein folding	54	51	3	207	7.1	−2.2
mRNA processing	53	51	2	210	7.0	−2.6
tRNA metabolic process	33	31	2	101	7.0	−1.3
mRNA metabolic process	59	55	4	236	6.9	−2.2
Intracellular transport	131	114	17	639	6.8	−2.5
Cellular component organization and biogenesis	377	309	68	2223	6.8	−4.0
Protein-RNA complex assembly	29	26	3	81	6.6	−0.4
Primary metabolic process	1024	724	300	6177	6.4	0.9
Metabolic process	1186	793	393	6890	6.4	6.2
Macromolecule complex assembly	67	61	6	297	6.1	−2.2
RNA splicing	44	41	3	172	6.1	−1.8
Establishment of cellular localization	146	126	20	771	6.1	−2.8
Cellular localization	147	127	20	788	5.9	−3.0
Response to heat	11	11	0	24	5.9	−1.1
Cellular metabolic process	1086	740	346	6440	5.8	3.9
Macromolecule metabolic process	827	633	194	5373	5.8	−5.0
Cellular component assembly	75	66	9	348	5.6	−1.9
ER-nuclear signaling pathway	10	10	0	22	5.5	−1.0
Protein metabolic process	452	354	98	2811	5.2	−3.4
Acrosome formation	3	3	0	3	5.2	−0.4
Pseudouridine synthesis	3	3	0	3	5.2	−0.4
RNA modification	8	8	0	17	5.1	−0.9

z-scores were calculated for each ontology category using GeneSifter® for all genes with a differential expression of 2.0 and $p < 0.05$. The ontologies were then sorted based on z-score for upregulated genes. The top 30 ontologies are listed here. ''List'' represents the number of genes for that ontology that meet the criteria of a fold-change >2.0 and $p < 0.05$. ''Array'' is the number of genes on the Affymetrix array that belong to the ontology group.

expression of genes associated with glucose homeostasis, the urea cycle, bilirubin production, ER stress, and redox balance to identify genes with transcripts that are significantly altered by pyrazole treatment. Expression of genes previously associated with altered transcription or mRNA stability of CYP2A5 were also examined. The effects of pyrazole on each of these specific pathways are described below. It should be noted that many lipid-associated genes were also differentially expressed, but these results will be published in a separate manuscript.

3.4. *Genes associated with glucose homeostasis and glycogen stores*

Since decreased serum glucose and hepatic glycogen depletion were observed in pyrazole-treated mice in this study we examined the effect of pyrazole on transcripts of genes involved in glucose and glycogen homeostasis. Sixty-five transcripts coding for proteins involved in carbohydrate metabolism were differentially expressed following pyrazole treatment. Since glucose homeostasis, lipid homeostasis, and energy metabolism are tightly interconnected, many of these genes have multiple cellular roles. For example, pyrazole upregulated the B2 non-catalytic subunit of AMP-activated protein kinase (Prkab2) approximately 10-fold. This gene has roles in regulating fatty acid oxidation, glycogen synthesis, fatty acid synthesis, and cellular ATP levels. Table 5 lists the genes specifically associated with glucose metabolism and storage as glycogen. Of these genes, seven were upregulated, eight were downregulated, and eight showed no change in mRNA expression. Transcript levels of several of these genes were confirmed by real-time RT-PCR. Glycogen synthase 2, Pck1, and glucokinase 1 were confirmed to be downregulated (8.4, 5.4, 2.6-fold, $p < 0.05$).

3.5. *Genes associated with the urea cycle and nitrogen metabolism*

For the downregulated genes, the KEGG pathway with the highest z-score of 6.37 was for ''Urea cycle and metabolism of amino groups''. Nineteen genes had a greater than 2-fold change in expression ($p < 0.05$), with 12 downregulated and 7 upregulated. Transcripts for the four major enzymes in the urea cycle were all decreased in pyrazole-treated mice, with decreases of 2.3, 3.1, 2.8, and 3.9-fold for carbamoyl-phosphate synthetase, argininosuccinate lyase, argininosuccinate synthetase 1, and ornithine transcarbamylase ($p < 0.05$). Guanidinoacetate methyltransferase which is involved in creatine synthesis was also strongly downregulated (5.5-fold) in pyrazole-treated mice. Upregulated genes included ornithine

Table 4 – Biological process ontologies for downregulated genes

Ontology	List	Up	Down	Array	z-up	z-down
Carboxylic acid metabolic process	132	51	81	457	0.8	13.5
Organic acid metabolic process	132	51	81	457	0.8	13.5
Monocarboxylic acid metabolic process	53	12	41	198	−1.9	10.8
Amino acid catabolic process	21	4	17	48	−0.4	10.1
Cellular lipid metabolic process	113	50	63	472	0.4	9.1
Amine catabolic process	25	8	17	57	1.0	9.0
Nitrogen compound catabolic process	25	8	17	57	1.0	9.0
Glutamine family amino acid biosynthetic process	11	3	8	15	1.3	8.9
Steroid biosynthetic process	23	5	18	64	−0.6	8.9
Lipid metabolic process	129	60	69	554	0.7	8.9
Amino acid and derivative metabolic process	91	46	45	290	3.4	8.8
Nitrogen compound metabolic process	103	51	52	371	2.4	8.6
Generation of precursor metabolites and energy	150	69	81	720	−0.4	8.6
Electron transport	92	39	53	390	−0.0	8.5
Amino acid metabolic process	74	36	38	236	2.7	8.4
Steroid metabolic process	37	11	26	129	−0.6	8.4
Amino acid biosynthetic process	21	8	13	40	2.1	8.3
Amine metabolic process	95	48	47	349	2.4	7.9
Proline catabolic process	3	0	3	3	−0.6	7.8
Lipid biosynthetic process	58	24	34	221	0.4	7.6
Glycine metabolic process	6	1	5	9	0.1	7.2
Arginine biosynthetic process	5	1	4	6	0.5	7.2
Cellular catabolic process	100	50	50	418	1.4	7.2
C21-steroid hormone metabolic process	7	0	7	17	−1.4	7.1
Aromatic compound catabolic process	7	1	6	13	−0.3	7.1
C21-steroid hormone biosynthetic process	6	0	6	13	−1.2	7.1
Alcohol metabolic process	60	27	33	234	0.8	6.9
Fatty acid metabolic process	33	9	24	143	−1.5	6.9
Gluconeogenesis	9	2	7	18	0.2	6.9
Cofactor metabolic process	53	24	29	193	1.1	6.9

z-scores were calculated for each ontology category using GeneSifter® for all genes with a differential expression of 2.0 and $p < 0.05$. The ontologies were then sorted based on z-score for downregulated genes. The top 30 ontologies are listed here.

decarboxylase (structural 1, 2.1-fold), spermidine synthase (3.1-fold), and spermidine/spermine N1-acetyl transferase 1 (3.2-fold).

3.6. *Genes associated with bilirubin levels*

Bilirubin is a degradation product of heme that can be elevated in the serum by hepatocellular damage, obstruction of the biliary tract, or hemolysis of red blood cells. Bilirubin production from heme involves two enzymes, heme oxygenase which converts heme to biliverdin and biliverdin reductase which converts biliverdin into bilirubin. Both of these enzymes were strongly upregulated by pyrazole treatment, with heme oxygenase upregulated by 6.8-fold and biliverdin reductase B upregulated by 5.6-fold. There was no significant change in mRNA levels of UDP-glucuronosyltransferase (Ugt1a1), the enzyme primarily responsible for conjugation of bilirubin.

3.7. *Pyrazole increases redox gene expression and markers of ER stress*

Treatment with pyrazole led to the elevation of many markers of cellular stress. These genes included transcription factors, markers of DNA damage, cell cycle genes, and genes associated with redox status (Table 6). Differential expression of several redox-associated genes was confirmed by real-time RT-PCR. The results of this analysis are shown in Fig. 2. Glutathione S-transferases alpha 1 and mu 1 were increased by more than 5-fold in pyrazole-treated mice. In addition, enzymes associated with glutathione production and oxidation status

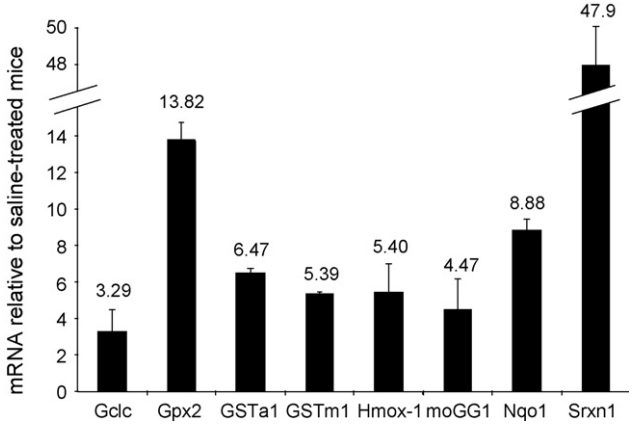

Fig. 2 – Pyrazole increases expression of multiple oxidative stress-responsive genes. Mice were treated with saline (not shown) or pyrazole (200 mg/kg) for 24 h and CYP2A5 mRNA levels were determined by comparative real-time RT-PCR as described in Section 2. All values are the average for four mice and significantly differ from saline-treated mice, $p < 0.05$.

Table 5 – Expression of glucose and glycogen homeostasis genes after pyrazole treatment

Unigene	Gene symbol	Gene name	Fold change
Gluconeogenesis			
Mm.1845	Pcx	Pyruvate carboxylase	−2.3
Mm.26686	Pck1	Phosphoenolpyruvate carboxykinase	−4.6
Mm.289741	Fbp1	Fructose 1,6-bisphosphatase	NC
Mm.589	Gpi	Glucose phosphate isomerase	NC
Mm.18064	G6pc	Glucose-6-phosphatase	−4.4
Glycogenolysis			
Mm.25692	Pygl	Liver glycogen phosphorylase	−3.0
Mm.2325	Pgm1	Phosphoglucomutase 1	+7.9
Mm.390201	Pgm3	Phosphoglucomutase 3	+2.1
Mm.237099	Agl	Debranching enzyme (amylo-1,6-glucosidase, 4-alpha-glucanotransferase)	NC
Glycolysis			
Mm.22035	Gck	Glucokinase	−2.6
Mm.269649	Pfkl	Phosphofructokinase, liver, B-type	−2.0
Mm.27583	Aldoa	Aldolase 1	+2.3
Mm.7729	Aldoc	Aldolase 3	−2.8
Mm.4222	Tpi1	Triose phosphate isomerase	NC
Mm.343110	Gapdh	Glyceraldehyde phosphate dehydrogenase	NC
Mm.717	Pgk2	Phosphoglycerate kinase	+1.6
Mm.61682	Pgam5	Phosphoglycerate mutase	+2.3
Mm.70666	Eno1	Enolase	NC
Mm.383180	Pklr	Pyruvate kinase, liver and red blood cell	NC
Glycogen synthesis			
Mm.28877	Ugp2	UDP-glucose pyrophosphorylase 2	NC
Mm.6375	Gyg	Glycogenin	+2.0
Mm.27597	Gys2	Glycogen synthase 2	−6.0
Mm.39610	Gbe1	Glycogen branching enzyme	+3.2

All fold changes are relative to saline controls and have a p-value <0.05. Genes that are involved in multiple pathways (e.g. glycolysis and gluconeogenesis) are only listed once. NC = no change.

were upregulated, including the catalytic subunit of glutamate-cysteine ligase (Gclc) and sulfiredoxin 1 (Srxn1). Several antioxidant/oxidative stress-associated enzymes were also confirmed to be upregulated including glutathione peroxidase (GPx2), heme oxygenase (Hmox1), and NADPH reductase quinone 1, and the DNA damage repair gene mOGG1 (Fig. 2). Comparison of the real-time RT-PCR and microarray results indicate that all genes were regulated in the same direction and to a similar magnitude for both assays.

Eighty-four of the stress gene transcripts upregulated by pyrazole were involved in the response to unfolded protein or ''endoplasmic reticulum (ER) stress'' (Table 7). Many of these transcripts are for genes encoding heat shock proteins and molecular chaperones involved in protein folding. Glucose-regulated protein 78 (Grp78, Hspa5), which was elevated 3.43-fold on the array, was confirmed by real-time RT-PCR (+3.8, $p < 0.05$) and Western blot analysis (+1.8, $p < 0.05$). Elevation of Grp94 was also confirmed by Western blot analysis and showed a 1.8-fold increase in protein levels ($p < 0.05$). In addition, multiple mRNA transcripts were upregulated for components of the ubiquitination pathway and the proteasomal complex.

3.8. *Pyrazole alters expression of several genes known to regulate CYP2A5 expression*

Cyp2a5 expression can be regulated both transcriptionally and post-transcriptionally. Transcriptional regulation of *Cyp2a5* has been associated with HNF4 [15], Oct-1 [15], AhR [16], Arnt [17], DBP [18], Pparα [19], and Nrf2 [20] expression. Messenger RNA levels for HNF4, Oct-1, or AhR were not altered 24-h after pyrazole treatment, but DBP was reduced more than 50-fold (−55.9), and Pparα was also decreased (2.2-fold). Arnt1 expression was increased (4.7-fold), and although Nrf2 levels were unchanged 24-h after treatment, multiple Nrf2-responsive genes were increased by pyrazole treatment. Post-transcriptional regulation of *Cyp2a5* via increased mRNA stability is associated with binding of hnRNPA1 [21]. For this study, hnRNPA1 was one of the multiple RNA processing genes upregulated by pyrazole treatment (2.4-fold).

3.9. *Effects of pyrazole on drug metabolizing enzymes*

Cyp2a5 and *Cyp2e1* are upregulated by pyrazole treatment, at the post-transcriptional and post-translational levels, respectively [21,22]. In this study we confirmed the repressive effects of pyrazole on mRNA expression of other enzymes involved in drug metabolism. As can be seen in Table 8, mRNAs for most CYP enzymes were strongly downregulated by pyrazole treatment with the exceptions of *Cyp2a5*, *Cyp2r1*, and *Cyp51* which were upregulated. Upregulation of *Cyp2a5* and *Cyp51* mRNA were confirmed by real-time RT-PCR with a 2.5-fold and 1.7-fold induction, respectively ($p < 0.05$), while downregulation of *Cyp7a1* (22-fold) was also confirmed. Regarding the Phase II enzymes, most glutathione S-transferases (GSTs) were upregulated, however, sulfotransferases were either

Table 6 – Stress-related genes regulated by pyrazole

Unigene	Gene symbol	Gene name	Fold change
Transcription factors			
Mm.641	Atf4	Activating transcription factor 4	+2.1
Mm.377046	Atf6	Activating transcription factor 6	+3.3
Mm.4068	Crebl1	CAMP responsive element binding protein-like 1	+2.0
Mm.273090	Cebpg	CCAAT/enhancer binding protein (C/EBP), gamma	+3.6
–	–	Tumor necrosis factor, alpha-induced protein 1 (endothelial)	+2.6
Mm.391700	Foxo3a	Forkhead box O3a	−2.6
Mm.259072	Ppargc1a	Peroxisome proliferative activated receptor, gamma, coactivator 1 alpha	−3.4
Mm.3020	Pparg	Peroxisome proliferators activated receptor gamma	+2.0
Cell redox homeostasis/oxidative stress			
Mm.404024	Dusp10	Dual specificity phosphatase 10	+4.7
Mm.9075	Ephx1	Epoxide hydrolase 1, microsomal	+2.3
Mm.89888	Gclc	Glutamate-cysteine ligase, catalytic subunit	+9.8
–	GPx2	Glutathione peroxidase	+7.4
Mm.283573	Gsr	Glutathione reductase 1	+3.4
Mm.252316	Gss	Glutathione synthetase	+3.2
Mm.276389	Hmox-1	Heme oxygenase 1	+6.8
–	Nqo1	NAD(P)H dehydrogenase, quinone 1	+6.1
Mm.263177	Pdia3	Protein disulfide isomerase associated 3	+4.3
Mm.2442	Pdia4	Protein disulfide isomerase associated 4	+3.9
Mm.222825	Pdia6	Protein disulfide isomerase associated 6	+4.6
Mm.347009	Prdx2	Peroxiredoxin 2	−2.5
Mm.116769	Qscn6l1	Quiescin Q6-like 1	+2.2
Mm.290876	Sod2	Superoxide dismutase 2, mitochondrial	−4.0
Mm.218639	Srxn1	Sulfiredoxin 1 homolog (*S. cerevisiae*)	+72.0
Mm.317701	Txndc4	Thioredoxin domain containing 4 (endoplasmic reticulum)	+2.2
Mm.19169	Txnl1	Thioredoxin-like 1	+2.1
Mm.210155	Txnrd1	Thioredoxin reductase 1	+4.0
DNA damage stimulus			
Mm.43612	Ogg1	8-Oxoguanine DNA-glycosylase 1	+2.5
Mm.332593	Alkbh2	AlkB, alkylation repair homolog 2 (*E. coli*)	+6.9
Mm.203	Apex1	Apurinic/apyrimidinic endonuclease 1	+3.5
Mm.272989	Asf1a	ASF1 anti-silencing function 1 homolog A (*S. cerevisiae*)	+2.2
Mm.235309	Bcl3	B-cell leukemia/lymphoma 3	+2.6
Mm.392646	Btg2	B-cell translocation gene 2, anti-proliferative	+2.5
Mm.110220	Ddit3	DNA-damage inducible transcript 3	+35.6
Mm.250841	Ddit4l	DNA-damage-inducible transcript 4-like	+2.3
Mm.280913	Eccr1	Excision repair cross-complementing rodent repair deficiency, complementation group 1	+2.0
Mm.389750	Gadd45a	Growth arrest and DNA-damage-inducible 45 alpha	+8.6
Mm.245931	H2afx	H2A histone family, member X	+3.7
Mm.277136	Lig3	Ligase III, DNA, ATP-dependent	+2.7
Mm.358657	Prpf19	PRP19/PSO4 pre-mRNA processing factor 19 homolog (*S. cerevisiae*)	+2.5
–	–	RAD1 homolog (*S. pombe*)	+3.5
Mm.103812	Rad18	RAD18 homolog (*S. cerevisiae*)	+2.3
Mm.341756	Rad51l1	RAD51-like 1 (*S. cerevisiae*)	+2.0
Mm.149	Rad52	RAD52 homolog (*S. cerevisiae*)	+2.3
–	–	Uracil DNA glycosylase	+7.0
Mm.37531	Xrcc4	X-ray repair complementing defective repair in Chinese hamster cells 4	+2.2
Cell cycle/apoptosis			
Mm.389890	Atf5	Activating transcription factor 5	+2.6
Mm.40038	Aifm3	Apoptosis-inducing factor, mitochondrion-associated 3	−2.0
Mm.239141	Bcl10	B-cell leukemia/lymphoma 10	+2.3
Mm.235309	Bcl3	B-cell leukemia/lymphoma 3	+2.6
Mm.378890	Bnip3	BCL2/adenovirus E1B interacting protein 1, NIP3	−3.5
Mm.84073	Bag3	Bcl2-associated athanogene 3	+5.7
Mm.19904	Bax	Bcl2-associated X protein	+2.7
Mm.141083	Bcl2l11	BCL2-like 11 (apoptosis facilitator)	+2.5
Mm.210125	Bmf	Bcl2-modifying factor	−11.8
Mm.3295	Bok	Bcl-2-related ovarian killer protein	−2.1
Mm.235081	Bid	BH3 interacting domain death agonist	+2.5
Mm.35687	Casp7	Caspase 7	−2.4

Table 6 (*Continued*)

Unigene	Gene symbol	Gene name	Fold change
Mm.10026	Cidec	Cell death-inducing DFFA-like effector c	+22.1
Mm.435554	Cideb	Cell death-inducing DNA fragmentation factor, alpha subunit-like effector B	−2.0
–	–	Cyclin D1	+5.7
Mm.195663	Cdkn1a	Cyclin-dependent kinase inhibitor 1A (P21)	+20.9
Mm.44963	Cdkl2	Cyclin-dependent kinase-like 2 (CDC2-related kinase)	+2.6
Mm.1639	Mcl1	Myeloid cell leukemia sequence 1	+3.0
Mm.204876	Nol3	Nucleolar protein 3 (apoptosis repressor with CARD domain)	+3.0
Mm.245395	Pten	Phosphatase and tensin homolog	−2.4
Mm.391419	Pawr	PRKC, apoptosis, WT1, regulator	+2.7
Mm.4139	Rtkn	Rhotekin	+3.0
Mm.222	Trp53	Transformation related protein 53	+3.3
Mm.215389	Trp53bp1	Transformation related protein 53 binding protein 1	+2.1
Mm.393018	Trpinp1	Transformation related protein 53 inducible nuclear protein 1	+2.9

All fold changes are relative to saline controls and have a p-value <0.05. Genes with multiple cellular roles are listed for only a single category.

unchanged or downregulated. The UDP:glucuronosyltransferases were mostly unchanged, with the exceptions of Ugt2b34, Ugt2b35, and Ugt2b37 which were upregulated.

4. Discussion

The objective of this study was to determine the effects of pyrazole on hepatic gene expression and to utilize the expression patterns to identify potential stimuli for the induction of *Cyp2a5*. Our study demonstrates that pyrazole affects the expression of a large number of genes involved in many cellular pathways. While this makes it difficult to fully comprehend the specific cellular effects attributable to pyrazole, examination of the affected gene ontologies does provide insight into the underlying causes of metabolic and histological changes observed in the liver following pyrazole treatment, particularly with regards to carbohydrate, urea, and bilirubin homeostasis. In addition, our study enables us to better understand the cellular conditions that exist when *Cyp2a5* is induced, allowing for the identification of several cellular pathways that could play a role in the regulation of *Cyp2a5* during cellular injury.

We have demonstrated that altered expression of genes involved in cellular metabolism and energy homeostasis is a major response to pyrazole treatment, and may partly explain the glycogen depletion observed in pericentral hepatocytes and reduced serum glucose following pyrazole exposure. ''Electron transport'' and ''Generation of precursor metabolites and energy'' were two of the most significant gene ontologies for downregulated genes, and many downregulated genes were associated with the mitochondria, which are swollen following pyrazole treatment [9]. Reduced cellular energy status can have significant consequences on expression of metabolic genes involved in lipid and carbohydrate homeostasis [23]. Pyrazole decreases mRNA levels of most genes involved in carbohydrate homeostasis. This may indicate that the energy required for glucose metabolism is not available following pyrazole treatment due to hepatocellular injury. Reduced gluconeogenesis and glycogen synthesis in particular could lead to the hypoglycaemia and glycogen depletion observed following pyrazole treatment.

It is also interesting to note that many of the enzymes in the glucose and glycogen homeostatic pathways that are downregulated by pyrazole are targets of the energy-sensing AMP-activated kinase (AMPK). AMPK activity is activated by a wide array of metabolic stresses, including hypoxia, ischemia, oxidative and hyperosmotic stresses, as well as exercise and glucose deprivation (reviewed by [24]). In general, activation of AMPK triggers catabolic pathways that produce ATP, while turning off anabolic pathways that consume ATP, to maintain cellular energy stores. Short-term overexpression of the active form of AMPK has been associated with decreased serum glucose as well as decreased glycolysis, gluconeogenesis, and glycogen synthesis [25]. Pyrazole also appears to have similar effects on carbohydrate homeostasis, and leads to increased mRNA levels of Prkab2, a non-catalytic subunit of AMPK that positively regulates AMPK activity. Interestingly, this subunit also contains a glycogen binding domain that targets the enzyme to glycogen, allowing it to be in close proximity to several of the genes that it modifies post-translationally [26]. In particular, downregulation of G6Pase and Pck1 by pyrazole may be a response of AMPK activation since AMPK has been shown to inhibit the transcription of these genes by several mechanisms. Therefore, altered expression of carbohydrate-related genes may reflect an imbalance in cellular energy homeostasis and conservation of ATP via regulation of AMPK. Regardless of the underlying mechanism of regulation, pyrazole clearly interferes with transcription of genes involved in carbohydrate homeostasis. This may be important with regards to *Cyp2a5* regulation since glucagon and fasting have previously been shown to increase expression of *Cyp2a5* [27].

Pyrazole also alters cellular processes other than energy homeostasis. Elevated bilirubin and decreased urea nitrogen have been observed in mouse serum following pyrazole treatment [9], and the effect of pyrazole on serum urea was confirmed in this study. Our results demonstrate that pyrazole likely alters blood urea nitrogen and bilirubin levels by influencing the mRNA levels of enzymes involved in these pathways. Four of the five major enzymes of the urea cycle, were downregulated by pyrazole treatment, which could result in reduced urea production. Conversely, pyrazole elevated the mRNA levels of both enzymes in the heme

Table 7 – ER stress-related genes upregulated by pyrazole treatment

Unigene	Gene symbol	Gene name	Fold change
Molecular chaperones and other genes involved in protein folding			
Mm.22626	Ahsa1	AHA1, activator of heat shock protein ATPase homolog 1 (yeast)	+2.1
Mm.196315	Calr3	Calreticulin 3	+2.5
Mm.247788	Cct2	Chaperonin subunit 2 (beta)	+2.2
Mm.282158	Cct5	Chaperonin subunit 5 (epsilon)	+2.7
Mm.289900	Cct7	Chaperonin subunit 7 (eta)	+3.5
Mm.178	Cryab	Crystallin, alpha B	+2.4
Mm.29760	Dnaja1	DnaJ (Hsp40) homolog, subfamily A, member 1	+2.2
Mm.52319	Dnaja4	DnaJ (Hsp40) homolog, subfamily A, member 4	+2.8
Mm.282092	Dnajb1	DnaJ (Hsp40) homolog, subfamily B, member 1	+5.5
Mm.248776	Dnajb10	DnaJ (Hsp40) homolog, subfamily B, member 10	+2.6
Mm.37516	Dnajb11	DnaJ (Hsp40) homolog, subfamily B, member 11	+2.9
Mm.290110	Dnajb6	DnaJ (Hsp40) homolog, subfamily B, member 6	+2.2
Mm.27432	Dnajb9	DnaJ (Hsp40) homolog, subfamily B, member 9	+2.3
Mm.21762	Dnajc10	DnaJ (Hsp40) homolog, subfamily C, member 10	+2.7
Mm.32550	Dnajc12	DnaJ (Hsp40) homolog, subfamily C, member 12	+2.1
Mm.354767	Dnajc18	DnaJ (Hsp40) homolog, subfamily C, member 18	+3.1
Mm.266312	Dnajc2	DnaJ (Hsp40) homolog, subfamily C, member 2	+3.2
Mm.30729	Fkbp11	FK506 binding protein 11	+8.9
Mm.278458	Fkbp1a	FK506 binding protein 1a	+2.5
Mm.330160	Hspa5 (Grp78)	Heat shock 70 kDa protein 5 (glucose-regulated protein)	+3.4
Mm.13849	Hspb1	Heat shock protein 1	+221.0
Mm.215667	Hspe1	Heat shock protein 1 (chaperonin 10)	+2.2
Mm.270681	Hsp110	Heat shock protein 110	+10.2
Mm.6388	Hspa1a	Heat shock protein 1A	+26.9
Mm.372314	Hspa1b	Heat shock protein 1B	+72.7
Mm.239865	Hspa4	Heat shock protein 4	+2.3
Mm.39330	Hspa4l	Heat shock protein 4 like	+3.1
Mm.290774	Hspa8	Heat shock protein 8	+3.1
Mm.21549	Hspb8	Heat shock protein 8	+3.0
Mm.209419	Hspa9	Heat shock protein 9	+2.1
Mm.341186	Hsp90aa1	Heat shock protein 90 kDa alpha (cytosolic), class A member 1	+9.8
Mm.2180	Hsp90ab1	Heat shock protein 90 kDa alpha (cytosolic), class B member 1	+2.8
Mm.87773	Hsp90b1	Heat shock protein 90 kDa beta (Grp94), member 1	+5.0
Mm.398647	Ppia	Peptidylprolyl isomerase A	+2.5
Mm.295252	Ppid	Peptidylprolyl isomerase D (cyclophilin D)	+3.3
Mm.26704	Stch	Stress 70 protein chaperone, microsome-associated, human homolog	+2.6
Mm.32019	Tcp1	T-complex protein 1	+2.5
Mm.28808	Pfdn4	Prefoldin 4	+2.4
Mm.262053	Vcp	Valosin containing protein	+2.5
Mm.431982	Npm3	Nucleoplasmin 3	+2.9
–	Derl1	Der1-like domain family, member 1	+3.0
Mm.340943	Ern1	Endoplasmic reticulum (ER) to nucleus signalling 1	+2.4
–	–	ER degradation enhancer, mannosidase alpha-like 1	+2.1
–	–	ERO1-like (*S. cerevisiae*)	+3.2
Ubiquitination and protein degradation			
Mm.288477	Psme3	Proteaseome (prosome, macropain) 28 subunit, 3	+2.6
Mm.2462	Psmc2	Proteasome (prosome, macropain) 26S subunit, ATPase 2	+2.5
Mm.289832	Psmc3	Proteasome (prosome, macropain) 26S subunit, ATPase 3	+2.3
Mm.29582	Psmc4	Proteasome (prosome, macropain) 26S subunit, ATPase, 4	+2.2
Mm.18472	Psmc6	Proteasome (prosome, macropain) 26S subunit, ATPase, 6	+2.4
Mm.260539	Psmd11	Proteasome (prosome, macropain) 26S subunit, non-ATPase, 11	+2.6
Mm.21667	Psmd12	Proteasome (prosome, macropain) 26S subunit, non-ATPase, 12	+2.3
Mm.218198	Psmd14	Proteasome (prosome, macropain) 26S subunit, non-ATPase, 14	+4.1
Mm.243234	Psmd2	Proteasome (prosome, macropain) 26S subunit, non-ATPase, 2	+2.1
Mm.12194	Psmd3	Proteasome (prosome, macropain) 26S subunit, non-ATPase, 3	+2.5
Mm.2261	Psmd4	Proteasome (prosome, macropain) 26S subunit, non-ATPase, 4	+2.6
Mm.270632	Psmd5	Proteasome (prosome, macropain) 26S subunit, non-ATPase, 5	+4.3
Mm.27591	Psmd6	Proteasome (prosome, macropain) 26S subunit, non-ATPase, 6	+2.1
Mm.18347	Psmd7	Proteasome (prosome, macropain) 26S subunit, non-ATPase, 7	+3.1
Mm.273152	Psmd8	Proteasome (prosome, macropain) 26S subunit, non-ATPase, 8	+2.7
Mm.121265	Psma1	Proteasome (prosome, macropain) subunit, alpha type 1	+2.4
Mm.252255	Psma2	Proteasome (prosome, macropain) subunit, alpha type 2	+2.0
Mm.30270	Psma4	Proteasome (prosome, macropain) subunit, alpha type 4	+2.2
Mm.208883	Psma5	Proteasome (prosome, macropain) subunit, alpha type 5	+2.5

Table 7 (*Continued*)

Unigene	Gene symbol	Gene name	Fold change
Mm.21728	Psma7	Proteasome (prosome, macropain) subunit, alpha type 7	+2.5
Mm.22233	Psmb2	Proteasome (prosome, macropain) subunit, beta type 2	+2.4
Mm.21874	Psmb3	Proteasome (prosome, macropain) subunit, beta type 3	+2.3
Mm.368	Psmb4	Proteasome (prosome, macropain) subunit, beta type 4	+2.3
Mm.8911	Psmb5	Proteasome (prosome, macropain) subunit, beta type 5	+2.7
Mm.332855	Pomp	Proteasome maturation protein	+2.2
Mm.275970	Uchl3	Ubiquitin carboxyl-terminal esterase L3 (ubiquitin thiolesterase)	+2.2
Mm.237594	Ufd1l	Ubiquitin fusion degradation 1 like	+2.8
Mm.28234	Ubr2	Ubiquitin protein ligase E3 component n-recognin 2	−2.3
Mm.329277	Usp14	Ubiquitin specific peptidase 14	+3.1
Mm.272770	Usp2	Ubiquitin specific peptidase 2	−24.2
Mm.30602	Usp22	Ubiquitin specific peptidase 22	+2.0
Mm.224935	Ube1dc1	Ubiquitin-activating enzyme E1-domain containing 1	+2.5
Mm.289795	Ubap1	Ubiquitin-associated protein 1	+2.5
Mm.405832	Ube4b	Ubiquitination factor E4B, UFD2 homolog (*S. cerevisiae*)	+2.6
Mm.337238	Ube2f	Ubiquitin-conjugating enzyme E2F (putative)	+2.2
Mm.384234	Ube2i	Ubiquitin-conjugating enzyme E2I	+2.1
Mm.3074	Ube2l3	Ubiquitin-conjugating enzyme E2L 3	+2.3
Mm.318133	Ube2u	Ubiquitin-conjugating enzyme E2U (putative)	−2.2
Mm.28917	Ufm1	Ubiquitin-fold modifier 1	+3.0
Mm.3979	Ubl4	Ubiquitin-like 4	+2.7

All fold changes are relative to saline controls and have a p-value <0.05. Genes with multiple cellular roles are listed for only a single category.

degradation pathway responsible for bilirubin production. Elevation of serum bilirubin following pyrazole treatment is interesting since recent evidence has demonstrated that CYP2A5 may play a role in the degradation of bilirubin [28]. In addition, many of the conditions that result in CYP2A5 overexpression, including hepatitis, heavy metal toxicity, and exposure to porphyrinogenic agents, lead to increased levels of heme oxygenase which can cause increases in bilirubin. Further studies are necessary to determine whether *Cyp2a5* expression is regulated by this substrate, and if hyperbilirubinemia could be the common mechanism for upregulation of CYP2A5 during hepatotoxicity.

Since CYP2A5 is upregulated during hepatotoxicity and hepatitis, we previously suggested that it is a stress-responsive enzyme [14], and that upregulation of CYP2A5 is likely a consequence of cellular injury. Pyrazole significantly elevated serum ALT, and altered the expression of many genes involved in cellular response to stress including cell cycle and apoptosis genes, DNA repair genes, and stress-associated transcription factors. In particular, multiple genes associated with RNA processing were overexpressed following pyrazole treatment, making this biological process the highest ranked gene ontology for upregulated genes. This is not surprising since repair of hepatic damage requires the production of new proteins and therefore the synthesis and processing of many RNA transcripts. Pyrazole also upregulates many genes involved in response to the accumulation of unfolded protein in the endoplasmic reticulum (ER stress), including chaperone proteins that promote protein folding, transporters that export damaged proteins from the ER, and ubiquitin and proteasomal pathways which target and degrade unfolded proteins. It is possible that *Cyp2a5* expression is regulated not by ER stress per se but by a specific ER stress stimulus. For example, stimulation of ER stress by thapsigargin, tunicamycin, and the calcium ionophore A23187 does not upregulate CYP2A5, suggesting that glycosylation of newly synthesized proteins and altered ER calcium homeostasis are not associated with CYP2A5 regulation [14]. However, upregulation of CYP2A5 by the ER stress-causing reducing agent *trans*-4,5-dihydroxy-1,2-dithiane (DTTox) has led to the suggestion that *Cyp2a5* may be regulated by stress conditions that alter ER redox status [14].

The potential involvement of altered redox status in the upregulation of CYP2A5 is consistent with evidence of increased ROS [29] and increased protein carbonyl levels [14] associated with pyrazole treatment. Our results indicate that many of the stress-responsive transcripts that are elevated following pyrazole treatment are associated with altered redox status, and it is important to note that many of the stress-associated transcripts upregulated in this study can be transcriptionally regulated by the electrophilic and oxidative stress-responsive transcription factor Nfe2l2 (Nrf2). These transcripts encode proteins including the catalytic subunit of glutamate-cysteine ligase, multiple glutathione S-transferases, glutathione peroxidase 2 (Gpx2), NADPH quinone oxidoreductase 1 (Nqo1), heme oxygenase, carbonyl reductase 3, and members of the proteasomal complex, the majority of which were upregulated in the current study. This corresponds with previous evidence that has shown that Nrf2 protein and mRNA are upregulated by pyrazole treatment [30]. The relative importance of the Nrf2 pathway in the regulation of *Cyp2a5* by pyrazole remains unclear since pyrazole primarily regulates *Cyp2a5* post-transcriptionally. However, recent work has shown that *Cyp2a5* is upregulated at the transcriptional level by cadmium through a mechanism involving Nrf2 [20]. We are currently investigating the importance of Nrf2 overexpression and altered cellular redox status in the regulation of *Cyp2a5* by pyrazole and other chemical inducers.

Finally, it is interesting to note that mRNA levels of some known regulators of *Cyp2a5* are altered following pyrazole treatment. Pparα was downregulated by pyrazole, which corresponds with previous evidence that Pparα decreases

Table 8 – Regulation of drug metabolizing enzymes by pyrazole

Unigene	Gene symbol	Gene name	Fold change
Cytochrome P450 enzymes			
Mm.1262	Cyp17a1	Cytochrome P450, family 17, subfamily a, polypeptide 1	−7.6
Mm.20764	Cyp2c29	Cytochrome P450, family 2, subfamily c, polypeptide 29	−2.2
Mm.42100	Cyp2c38	Cytochrome P450, family 2, subfamily c, polypeptide 38	−6.6
Mm.329866	Cyp2c44	Cytochrome P450, family 2, subfamily c, polypeptide 44	−2.9
Mm.379575	Cyp2c54	Cytochrome P450, family 2, subfamily c, polypeptide 54	−7.4
Mm.157435	Cyp2d22	Cytochrome P450, family 2, subfamily d, polypeptide 22	−3.8
Mm.378904	Cyp2d9	Cytochrome P450, family 2, subfamily d, polypeptide 9	−2.4
Mm.4515	Cyp2f2	Cytochrome P450, family 2, subfamily f, polypeptide 2	−2.3
Mm.38963	Cyp2c37	Cytochrome P450, family 2, subfamily c, polypeptide 37	−7.0
Mm.332844	Cyp3a11	Cytochrome P450, family 3, subfamily a, polypeptide 11	−6.9
Mm.384461	Cyp3a25	Cytochrome P450, family 3, subfamily a, polypeptide 25	−2.5
Mm.379071	Cyp3a41	Cytochrome P450, family 3, subfamily a, polypeptide 41	−2.3
Mm.376968	Cyp39a1	Cytochrome P450, family 39, subfamily a, polypeptide 1	−5.0
Mm.426027	Cyp4f14	Cytochrome P450, family 4, subfamily f, polypeptide 14	−3.7
Mm.26539	Cyp4f15	Cytochrome P450, family 4, subfamily f, polypeptide 15	−4.6
Mm.245297	Cyp4v3	Cytochrome P450, family 4, subfamily v, polypeptide 3	−4.5
Mm.57029	Cyp7a1	Cytochrome P450, family 7, subfamily a, polypeptide 1	−18.7
Mm.20889	Cyp8b1	Cytochrome P450, family 8, subfamily b, polypeptide 1	−3.3
Mm.389848	Cyp2a5	Cytochrome P450, family 2, subfamily a, polypeptide 5	+3.6
Mm.108037	Cyp2r1	Cytochrome P450, family 2, subfamily r, polypeptide 1	+2.1
Mm.140158	Cyp51	Cytochrome P450, family 51	+2.3
Phase II enzymes			
Mm.9075	Ephx1	Epoxide hydrolase 1, microsomal	+2.3
Mm.197422	Gsta1	Glutathione S-transferase, alpha 1 (Ya)	+22.1
Mm.394593	Gsta3	Glutathione S-transferase, alpha 3	−5.0
Mm.304899	Gstcd	Glutathione S-transferase, C-terminal domain containing	+3.2
Mm.267014	Gstk1	Glutathione S-transferase kappa 1	−2.5
Mm.37199	Gstm1	Glutathione S-transferase, mu 1	+9.8
Mm.31203	Gstm4	Glutathione S-transferase, mu 4	+17.1
Mm.2746	Gstt1	Glutathione S-transferase, theta 1	−2.5
Mm.5731	Gstt3	Glutathione S-transferase, theta 3	−2.8
Mm.368982	Sult1a1	Sulfotransferase family 1A, phenol-preferring, member 1	−4.1
Mm.23502	Sult1b1	Sulfotransferase family 1B, member 1	−2.7
Mm.6824	Sult1d1	Sulfotransferase family 1D, member 1	−19.9
Mm.6562	Sult5a1	Sulfotransferase family 5A, member 1	−3.3
Mm.281844	Ugt2b34	UDP-glucuronosyltransferase 2 family, polypeptide B34	+2.3
Mm.312095	Ugt2b35	UDP-glucuronosyltransferase 2 family, polypeptide B35	+3.4
Mm.160362	Ugt2b37	UDP-glucuronosyltransferase 2 family, polypeptide B37	+4.5

All fold changes are relative to saline controls and have a p-value <0.05.

expression of CYP2A5 [19]. In addition, recent evidence demonstrates that a homodimer of the aryl hydrocarbon receptor nuclear translocator (Arnt) can upregulate CYP2A5, and expression of Arnt is required for the full activity of the *Cyp2a5* promoter [17]. Arnt mRNA levels were increased just under 5-fold by pyrazole treatment in the current study. Perhaps most importantly, considering that pyrazole primarily upregulates CYP2A5 at a post-transcriptional level, hnRNPA1 overexpression occurs with pyrazole treatment, along with many other RNA processing genes. Therefore, it is possible that several known regulators of *Cyp2a5* that are affected by pyrazole treatment may work in concert to increase expression of CYP2A5.

In conclusion, pyrazole regulates many cellular pathways affecting glucose and energy homeostasis, urea balance, and bilirubin production transcriptionally or post-transcriptionally. Future experiments are required to confirm that gene expression changes observed at the mRNA level in this study also result in changes at the protein and activity levels, to prove that these changes are responsible for the metabolic and physiological effects of pyrazole. Based on current knowledge of *Cyp2a5* regulation and results from this study, several pathways have been identified that may play a role in the regulation of *Cyp2a5* during hepatotoxicity. Further studies are needed to investigate the relative importance of impaired energy homeostasis, hyperbilirubinemia, ER stress, and redox imbalance in the regulation of *Cyp2a5* expression. Identification of the stimulus and regulatory mechanism(s) of *Cyp2a5* expression may also aid in identifying the functional role of CYP2A5 during hepatotoxicity.

Acknowledgements

This research was supported by the Natural Sciences and Engineering Research Council of Canada (NSERC). Kathleen Nichols is the recipient of funding from NSERC and the Ontario Ministry of Training, Colleges and Universities.

REFERENCES

[1] Camus AM, Geneste O, Honkakoski P, Bereziat JC, Henderson CJ, Wolf CR, et al. High variability of nitrosamine metabolism among individuals: role of cytochromes P450 2A6 and 2E1 in the dealkylation of *N*-nitrosodimethylamine and *N*-nitrosodiethylamine in mice and humans. Mol Carcinog 1993;7:268–75.

[2] Felicia ND, Rekha GK, Murphy SE. Characterization of cytochrome P450 2A4 and 2A5-catalyzed 4-(methylnitrosamino)-1-(3-pyridyl)-1-butanone (NNK) metabolism. Arch Biochem Biophys 2000;384:418–24.

[3] Pelkonen P, Lang MA, Negishi M, Wild CP, Juvonen RO. Interaction of aflatoxin B1 with cytochrome P450 2A5 and its mutants: correlation with metabolic activation and toxicity. Chem Res Toxicol 1997;10:85–90.

[4] Siu EC, Wildenauer DB, Tyndale RF. Nicotine self-administration in mice is associated with rates of nicotine inactivation by CYP2A5. Psychopharmacology (Berl) 2006;184:401–8.

[5] Sipowicz MA, Chomarat P, Diwan BA, Anver MA, Awasthi YC, Ward JM, et al. Increased oxidative DNA damage and hepatocyte overexpression of specific cytochrome P450 isoforms in hepatitis of mice infected with Helicobacter hepaticus. Am J Pathol 1997;151:933–41.

[6] Kobliakov V, Kulikova L, Samoilov D, Lang MA. High expression of cytochrome P450 2a-5 (coumarin 7-hydroxylase) in mouse hepatomas. Mol Carcinog 1993;7:276–80.

[7] Kojo A, Viitala P, Pasanen M, Pelkonen O, Raunio H, Juvonen R. Induction of CYP2A5 by pyrazole and its derivatives in mouse primary hepatocytes. Arch Toxicol 1998;72:336–41.

[8] Aida K, Negishi M. Posttranscriptional regulation of coumarin 7-hydroxylase induction by xenobiotics in mouse liver: mRNA stabilization by pyrazole. Biochemistry 1991;30:8041–5.

[9] Lieber CS, Rubin E, DeCarli LM, Misra P, Gang H. Effects of pyrazole on hepatic function and structure. Lab Invest 1970;22:615–21.

[10] Gilmore WJ, Hartmann G, Piquette-Miller M, Marriott J, Kirby GM. Effects of lipopolysaccharide-stimulated inflammation and pyrazole-mediated hepatocellular injury on mouse hepatic Cyp2a5 expression. Toxicology 2003;184:211–26.

[11] Wu Z, LeBlanc R, Irizarry RA. ''Stochastic models based on molecular hybridization theory for short oligonucleotide microarrays''. Johns Hopkins University, Dept. of Biostatistics Working Papers. Working Paper 4. http://www.bepress.com/jhubiostat/paper4; September 2003.

[12] Reiner A, Yekutieli D, Benjamini Y. Identifying differentially expressed genes using false discovery rate controlling procedures. Bioinformatics 2003;19:368–75.

[13] Doniger SW, Salomonis N, Dahlquist KD, Vranizan K, Lawlor SC, Conklin BR. MAPPFinder: using Gene Ontology and GenMAPP to create a global gene-expression profile from microarray data. Genome Biol 2003;4:R7.

[14] Gilmore WJ, Kirby GM. Endoplasmic reticulum stress due to altered cellular redox status positively regulates murine hepatic CYP2A5 expression. J Pharmacol Exp Ther 2004;308:600–8.

[15] Ulvila J, Arpiainen S, Pelkonen O, Aida K, Sueyoshi T, Negishi M, et al. Regulation of Cyp2a5 transcription in mouse primary hepatocytes: roles of hepatocyte nuclear factor 4 and nuclear factor I. Biochem J 2004;381:887–94.

[16] Arpiainen S, Raffalli-Mathieu F, Lang MA, Pelkonen O, Hakkola J. Regulation of the Cyp2a5 gene involves an aryl hydrocarbon receptor-dependent pathway. Mol Pharmacol 2005;67:1325–33.

[17] Arpiainen S, Lamsa V, Pelkonen O, Yim SH, Gonzalez FJ, Hakkola J. Aryl hydrocarbon receptor nuclear translocator and upstream stimulatory factor regulate cytochrome P450 2a5 transcription through a common E-box site. J Mol Biol 2005;67:1325–33.

[18] Lavery DJ, Lopez-Molina L, Margueron R, Fleury-Olela F, Conquet F, Schibler U, et al. Circadian expression of the steroid 15 alpha-hydroxylase (Cyp2a4) and coumarin 7-hydroxylase (Cyp2a5) genes in mouse liver is regulated by the PAR leucine zipper transcription factor DBP. Mol Cell Biol 1999;19:6488–99.

[19] Barclay TB, Peters JM, Sewer MB, Ferrari L, Gonzalez FJ, Morgan ET. Modulation of cytochrome P-450 gene expression in endotoxemic mice is tissue specific and peroxisome proliferator-activated receptor-alpha dependent. J Pharmacol Exp Ther 1999;290:1250–7.

[20] Abu-Bakar A, Lamsa V, Arpiainen S, Moore MR, Lang MA, Hakkola J. Regulation of CYP2A5 gene by the transcription factor nuclear factor (erythroid-derived 2)-like 2. Drug Metab Dispos 2007;35:787–94.

[21] Glisovic T, Soderberg M, Christian K, Lang M, Raffalli-Mathieu F. Interplay between transcriptional and post-transcriptional regulation of Cyp2a5 expression. Biochem Pharmacol 2003;65:1653–61.

[22] Winters DK, Cederbaum AI. Time course characterization of the induction of cytochrome P-450 2E1 by pyrazole and 4-methylpyrazole. Biochim Biophys Acta 1992;1117:15–24.

[23] Desvergne B, Michalik L, Wahli W. Transcriptional regulation of metabolism. Physiol Rev 2006;86:465–514.

[24] Long YC, Zierath JR. AMP-activated protein kinase signaling in metabolic regulation. J Clin Invest 2006;116:1776–83.

[25] Foretz M, Ancellin N, Andreelli F, Saintillan Y, Grondin P, Kahn A, et al. Short-term overexpression of a constitutively active form of AMP-activated protein kinase in the liver leads to mild hypoglycemia and fatty liver. Diabetes 2005;54:1331–9.

[26] Polekhina G, Gupta A, Michell BJ, van Denderen B, Murthy S, Feil SC, et al. AMPK beta subunit targets metabolic stress sensing to glycogen. Curr Biol 2003;13:867–71.

[27] Viitala P, Posti K, Lindfors A, Pelkonen O, Raunio H. cAMP mediated upregulation of CYP2A5 in mouse hepatocytes. Biochem Biophys Res Commun 2001;280:761–7.

[28] Abu-Bakar A, Moore MR, Lang MA. Evidence for induced microsomal bilirubin degradation by cytochrome P450 2A5. Biochem Pharmacol 2005;70:1527–35.

[29] Lu Y, Wang X, Cederbaum AI. Lipopolysaccharide-induced liver injury in rats treated with the CYP2E1 inducer pyrazole. Am J Physiol Gastrointest Liver Physiol 2005;289:G308–19.

[30] Gong P, Cederbaum AI. Nrf2 is increased by CYP2E1 in rodent liver and HepG2 cells and protects against oxidative stress caused by CYP2E1. Hepatology 2006;43:144–53.